INTERNATIONAL SOCIETY FOR SOIL MECHANICS AND GEOTECHNICAL ENGINEERING



This paper was downloaded from the Online Library of the International Society for Soil Mechanics and Geotechnical Engineering (ISSMGE). The library is available here:

https://www.issmge.org/publications/online-library

This is an open-access database that archives thousands of papers published under the Auspices of the ISSMGE and maintained by the Innovation and Development Committee of ISSMGE.

The paper was published in the proceedings of the 20th International Conference on Soil Mechanics and Geotechnical Engineering and was edited by Mizanur Rahman and Mark Jaksa. The conference was held from May 1st to May 5th 2022 in Sydney, Australia.

3D nonlinear seismic response analyses of nuclear island structure in soft deposits

Analyse de la réponse sismique non linéaire 3D d'un bâtiment d'île nucléaire dans des dépôts mous

Chen Guoxing, Zhu Shengdong, Chen Weiyun & Wang Yanzhen *Institute of Geotechnical Engineering, Nanjing Tech University, China, gxc6307@163.com*

ABSTRACT: The safety of the nuclear island (NI) constructed in soft deposits that are subject to strong earthquakes is becoming an engineering challenge. An example of one such NI is the AP1000 NI located in the coastal deposits, China. Using the three-dimensional (3D) finite element method, a nonlinear seismic response analysis of a pile-raft-supported AP1000 NI was developed. In the response analysis, the engineering geology characteristics, nonlinear dynamic behavior of soils, and artificial boundary conditions are considered. The spectral accelerations (SAs) of the NI structure are more intense when the bedrock motion frequency components are close to the basic frequency of the main structure of the NI, and the SA predominant periods are almost the same as those of the bedrock motions. The peak acceleration amplification factors (PAAFs) and the peak relative displacements (PRDs) both increase with the increasing heights. For the near-field and far-field strong earthquakes, respectively, the PAAFs are mainly dependent on the NI itself and the seismic wave propagating from the bedrock to the NI base. The PRDs to the far-field earthquakes are more intense. With the increasing peak bedrock accelerations, the PAAFs and PRDs of the NI structure decrease and increase, respectively.

RÉSUMÉ: La sécurité de l'Îles Nucléaires (IN) construite dans des dépôts mous affecté par des forts tremblements de terre devient un défi dans la domaine d'ingénierie. Un exemple de IN est l'AP1000 situé dans les dépôts littoraux de la Chine. En utilisant la méthode d'élément limitée en trois dimensions (3D), la réponse sismique non linéaire de l'AP1000 NI supporté par des radeaux de pile est developpée. Dans l'analyse de la réponse, les caractéristiques géologiques techniques, les effets dynamiques non linéaires du sol et les limites artificielles sont prises en compte. Les accélérations spectrales (SAs) de la structure IN sont plus forte pour la composante de fréquence du mouvement du soubassement près de la fréquence basique de la structure principale de l'IN, et sa période prédominante de SAs est presque identique que le mouvement du soubassement. Le facteur d'amplification de l'accélération de crête (FAACs) et le déplacement relatif de crête (DRCs) augmentent avec l'augmentation de l'hauteur. Pour le fort tremblement de terre du champ proche et du champ lointain, respectivement, le FAACs dépend principalement de IN lui-même et l'onde des séismes qui se propagent du soubassement à la base de IN. Le DRCs aux tremblements de terre en champ lointain est plus forte. Avec l'augmentation de l'accélération de la crête du soubassement, le FAACs et le DRCs de la structure IN diminuent et augmentent respectivement.

KEYWORDS: soft deposits; nuclear island structure; pile-raft foundation; soil nonlinear; seismic response

1 INTRODUCTION

With the rapid development of the nuclear power industry, there are fewer and fewer high-quality bedrock sites for nuclear power plants. Scholars have studied the effect of soil-structure interaction (SSI) on the seismic response of NI structures.

Tunon-Sanjur et al. (2007) built four kinds of finite element (FE) models of AP1000 NI and used the equivalent linear model to simulate the nonlinearity of soil. With Consideration of the SSI effect, the floor response spectra of different models under various site conditions were compared and analyzed. Saxena et al. (2012) investigated the influence of the SSI effect on the seismic response of the containment structure with different embedded depths by considering slip and detachment of the contact surface. In this study, the equivalent plane stress finite element model was established to simulate the containment structure, and the soil was regarded as elastic. Wang et al. (2017) analyzed the seismic response of the HTR-10 nuclear reactor by building a refined three-dimensional finite element model, they explored the influence of the SSI effect on the seismic response of the HTR-10 nuclear reactor and suggested that the distance between the truncation boundary of the site and the nuclear reactor should not be less than three times the size of the nuclear reactor. Yin et al. (2017) took the response of one-dimensional site analysis using the equivalent linear method as the input motion, then they carried out the seismic response analysis of the CPR1000 NI structure on a soil site. This method is efficient and convenient yet can only partly reflect the actual nonlinear behavior of the soils and structure. By contrast, taking the structure and soil site as a whole, then directly performing a dynamic analysis of the whole model is a better way for analyzing the seismic characteristics of the NI structure considering the SSI effect. Wang et al. (2013) employed this whole-model method for a 3D seismic analysis of the AP1000 NI structure. The results show that the influence of the SSI effect cannot be overlooked when the soil conditions are poor.

Most of the previous researches on the seismic response characteristics of the NI structures on soil sites employed the equivalent linear method for the soil material. On the other hand, some treat the soil as an equivalent viscoelastic instead of a true nonlinear material. Both of these methods will neglect the secondary nonlinearity of the soil derived from SSI.

Due to the limitation of site selection, some nuclear power plants can only be built on soft soil sites with piles reinforced. Therefore, it is of great practical significance to explore the influence of soil-pile foundation-NI structure interaction (SPSI) on the seismic response of the NI structure. The existence of the SPSI effect will directly affect the dynamic characteristics of the structure and the soil site. As far as the seismic safety of the NI structure is concerned, this influence deserves to be highlighted.

Based on the ABAQUS platform, a three-dimensional finite element model of the soft soil-pile-raft foundation-NI structure system is established in this paper. The bedrock input motions with different characteristics are selected and loaded, and the true nonlinearity of soil is considered so the seismic response characteristics of the AP1000 NI structure can be revealed and studied. The conclusions are of important reference value to the seismic design of AP1000 NI structure on soft soil site.

2 MODELING OF THE NUCLEAR ISLAND STRUCTURE

2.1 Profile of AP1000 nuclear power plant

AP1000, an abbreviation for the Advanced Passive Pressurized Water Reactor with a power level of 1000 MWe which is developed by Westinghouse, is standardized design and equipped with the advanced III⁺ nuclear power technology. AP1000 is mainly composed of five parts: NI, steam turbine building, auxiliary building, diesel generator plant, and radioactive waste building, as shown in Figure 1. The NI is the most important supporting structure, consisting of the containment building (steel containment vessel and internal structure), the shield building, and the auxiliary building, which are all located on a thick raft. The top of the shield building is equipped with a cooling system water tank. The water spraying from the water tank cools the temperature of the steel containment when the accident occurs. The volume and mass of the water tank are about 3000 m³ and 3000 t, respectively.

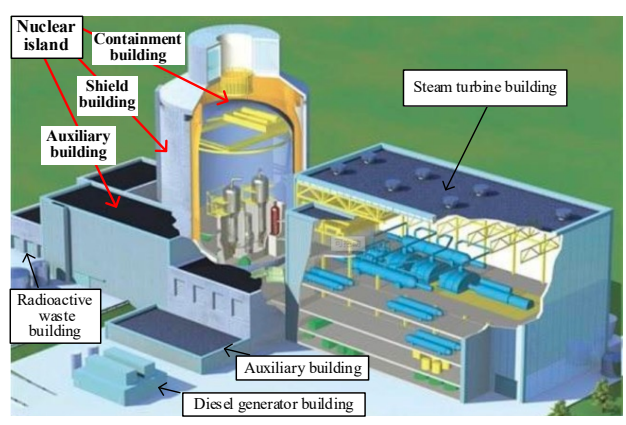


Figure 1 The structural components of the AP1000 nuclear power plant

2.2 The nuclear island structure model

According to the AP1000 design control (Westinghouse, 2009), a standardized simplified centralized mass-stick model is established. The three-dimensional (3D) concentrated mass-stick model represents the steel containment and its internal structure, the shield building, and the auxiliary building (Figure 2(b)), which is mainly composed of discrete concentrated mass points, elastic structural sticks, and rigid beam elements. The discrete concentrated masses are set at the main floor elevations and discontinuous positions of the structure, and the eccentricity between the structural rigidity center and the mass center is also considered. The eccentricity of the structure is simulated by the horizontal rigid beam elements by connecting the concentrated mass to the vertical elastic structural elements. The discrete components and subsystems in the 3D concentrated mass-stick model are connected by rigid beam elements (existing in the form of the rigid constraints, the yellow line segment in Figure 2(b). Due to the irregular geometric configuration of AP1000, the performance parameters of the 3D concentrated mass-stick model are determined by the method of extracting the structural section from the 3D finite element model. The overall model of the NI structure couples the reactor coolant loop system and the sub-systems of the containment internal structure (Figure

2(b)); the masses of other sub-systems and equipment are merged into the corresponding centralized masses.

On the ABAQUS platform, the model of the NI structure is established according to the end coordinates, material properties, element parameters, element type information, cross-section information, component characteristics, and constraints. The 3D AP1000 concentrated mass-stick model includes 203 structural components and 110 concentrated masses points (with 15 beam units and 14 concentrated masses for the containment, and with 10 beam units and 14 concentrated mass units for the shield building). The constraint relationships among the various components of the NI structure model are extremely complicated, including 406 constraint equations in total.

Due to the non-negligible size of the water tank, the water in the tank will affect the dynamic characteristics of the NI structure. When the NI structure is subjected to strong ground motions, the inertia and sloshing effects of the water in the tank will affect the safety of the NI structure (Zhao & Chen, 2014).

The influence of water in the tank on the seismic response of the NI structure is mainly manifested in the additional mass and hydrodynamic pressure. The additional mass will reduce the fundamental frequency of the NI structure; the hydrodynamic pressure caused by the earthquake includes the pressure caused by the inertia of the water and the pressure caused by the water sloshing, which acts on the water-structure interface and is transmitted to the NI structure. Housner (1957) assumed that the tank wall is rigid, and the water in the tank can be regarded as an incompressible ideal liquid, meanwhile, a 3D equivalent massspring system is used to simulate the effects of impact pressure and sloshing pressure. Similarly, Zhao & Chen (2014) made the equivalent mass of the impact pressure and sloshing pressure fixed at the respective equivalent height above the bottom of the water tank. This paper, integrating the equivalent impact mass of water into the concentrated mass of the shield building corresponding to the top and bottom of the water tank (Node 310, 309). The equivalent concentrated mass point Node 312 (311) is connected to the shield building Node 310 (309) through the zero-length connector to simulate the effect of the water sloshing.

2.3 Reliability analysis of the nuclear island model

For the validation of the 3D AP1000 NI concentrated mass-stick ABAQUS model, we built an AP1000 NI structure in ANSYS for modal analysis. Then comparing the modal frequencies of these two models. Table 1 shows the 1st to 15th sets of the frequencies that reflect the overall structural characteristics of the AP1000 NI. The first 6 sets of the frequencies mainly reflect the vibration of the 3D concentrated mass point-spring system for the tank on the top of the shield building and the sloshing water in the tank, and the 7th to 15th sets of the frequencies reflect the natural vibration characteristics of t

he main supporting structure of the NI. It can be seen that the modal analysis results of the two models are very close, which ensures the reliability of the ABAQUS model.

3 MODELING OF THE FOUNDATION AND THE SITE

The proposed AP1000 NI site is mainly composed of silty clay, partially silty sand. The simplified soil layer profile is shown in Figure 3, and the site soil layer information is shown in Table 2. The soil layer is regarded as an infinite horizontal extension in the direction out of the profile plane. The horizontal size of the site model is about 5 times the size of the raft, and the viscoelastic artificial boundary is set at the four-side lateral boundary (Liu & Li 2005; Liu et al., 2006). The underlying dense basalt layer with a shear wave velocity of about 2500 m/s is selected as the seismic bedrock, which is regarded as a rigid boundary.

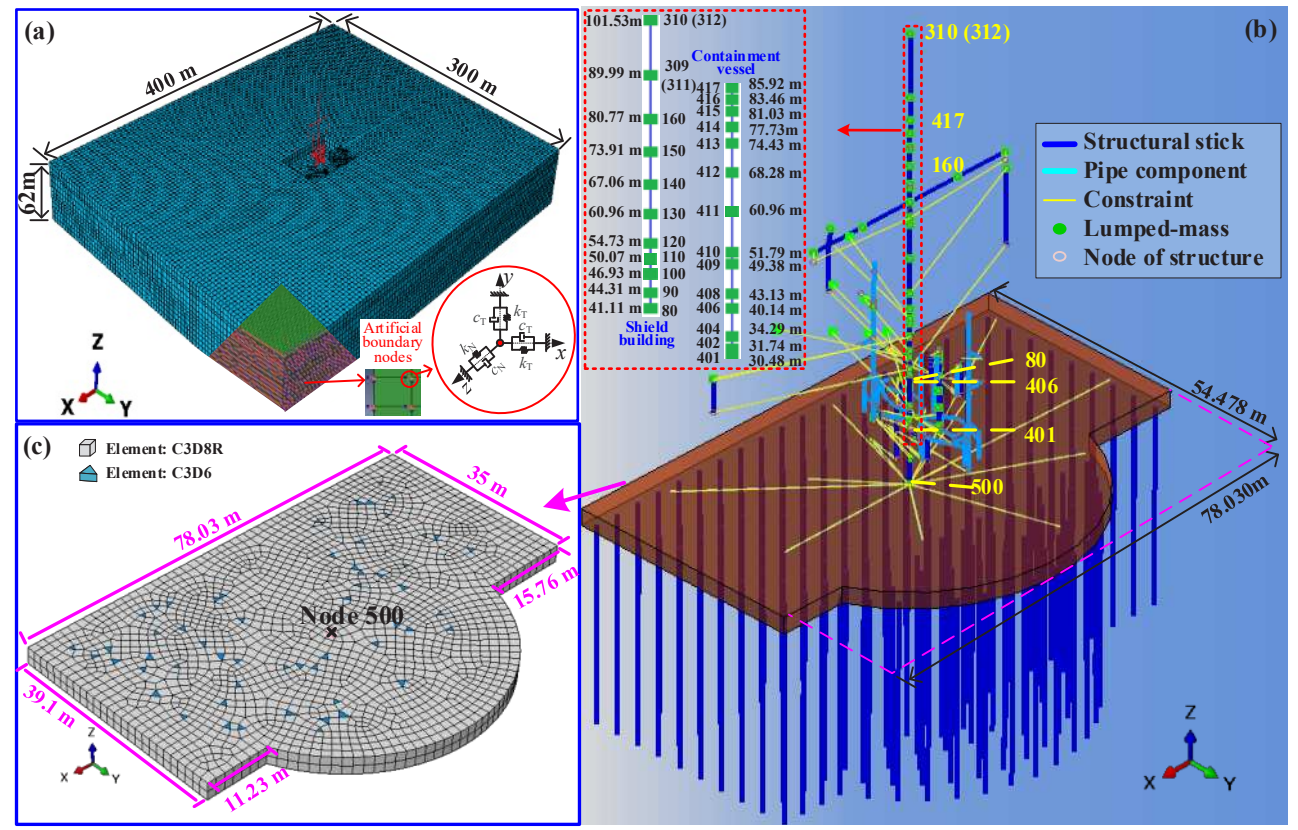


Figure 2 Overview diagrams of the soil-pile-raft foundation-AP1000 nuclear island structure system for finite element modeling

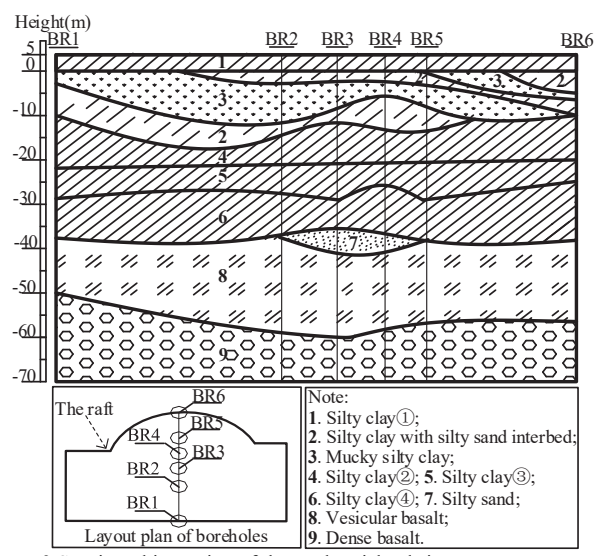


Figure 3 Stratigraphic section of the nuclear island site

The fact that the shallow layers of soils are quite soft, so the pile-raft foundation is adopted for reinforcement. The raft is 3 m thick, and the pile tops and bottoms are embedded in the raft for 0.15 m and the basalt for 2 m, respectively. The meshing of the raft can be seen in Figure 2(c). There is a total of 230 piles, which are evenly distributed. The diameter and the length for each pile are 1.5 m and 36 m, respectively. The material for the pile-raft foundation is simulated with C40 concrete and is regarded as elastic. The 8-node linear brick elements with reduced integration (C3D8R) in ABAQUS are selected to simulate the soil and the raft. Moreover, the spatial two-node linear beam element (B31) is selected to simulate the piles, each with 20 elements. Figure 2(a) shows the ABAQUS model of the soil-foundation-NI structure system.

Table 1 Comparison of the modal frequencies for ABAQUS and ANSYS modeling of the nuclear island structure

Modal	Modal frequency/ Hz				
set	ANSYS	ABAQUS			
1	0.13553	0.15575			
2	0.13554	0.15590			
3	0.13556	0.15603			
4	0.13556	0.15603			
5	0.81199	0.79388			
6	0.83214	0.86469			
7	2.8796	2.90979			
8	3.0185	2.93329			
9	3.6043	3.52113			
10	4.1078	4.2161			
11	4.1588	4.2446			
12	5.1992	4.8465			
13	5.2133	4.8657			
14	5.9276	5.4171			
15	6.4047	6.1767			

3.1 Dynamic constitutive model of soil

To describe the dynamic nonlinear behavior characteristics of the soils, Zhao et al. (2017) developed an irregular loading and unloading rule based on the Davidenkov skeleton curve. The Davidenkov skeleton curve can be expressed as below:

$$\tau = F_{\rm b}(\gamma) = G_{\rm max} \gamma \Big[1 - H(\gamma) \Big] \tag{1}$$

where τ is shear stress; G_{max} is initial shear modulus; $F_{\text{b}}(\gamma)$ is the function for generalized hyperbolic backbone curve with shear strain γ ; $H(\gamma)$ is the function for the shape of stress-strain relationship, expressed as follows:

$$H(\gamma) = \left\{ \frac{\left(\gamma / \gamma_{\rm r}\right)^{2\rm B}}{1 + \left(\gamma / \gamma_{\rm r}\right)^{2\rm B}} \right\}^{\rm A} \tag{2}$$

where A and B are the fitting parameters for adjusting the shape of the backbone curve in characterizing the nonlinear behavior of soils and γ_r is the reference shear strain.

In this paper, the original soil samples were taken from the proposed NI site, and the corresponding test data were obtained from the resonant column test. Figure 4 shows the test curves of the dynamic shear modulus ratio $G/G_{\rm max}$ and the damping ratio λ of the site soil and the corresponding parameters are listed in Table 2.

The constitutive model has shown strong applicability through good applications of the nonlinear seismic response analysis of large-scale seabed site (Ruan et al., 2019), submarine tunnel (Chen et al., 2020), underground structure (Miao et al., 2018), and NI structure on soft rock (Li and Chen, 2020).

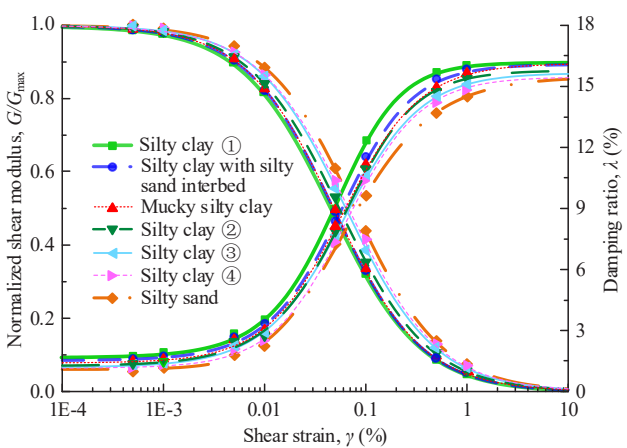


Figure 4 Shear modulus reduction and damping ratio increasing curves of the site soils

Table 2 The parameters of the soils

No	Soil	S-wave velocity (m/s)	Density (kg/m³)	Constitutive model parameters		
				A	В	$\gamma_{\rm r}$ (×10 ⁻⁴)
1	Silty clay①	105	1810	1.03	0.47	5.28
2	Silty clay with silty sand interbed	102	1900	1.01	0.45	6.04
3	Mucky silty clay	239	1930	1.03	0.46	5.9
4	Silty clay2	237	1890	1.03	0.45	6.01
5	Silty clay®	254	1940	1.04	0.45	6.61
6	Silty clay4	325	1960	1.06	0.44	7.41
7	Silty sand	346	2010	1.08	0.44	8.29
8	Vesicular basalt	1360	2620	1.20	0.40	10.50

3.2 Site and foundation finite element model

According to the research of Kuhlemeyer & Lysmer (1973), the element size should be $1/8 \sim 1/10$ of the wavelength corresponding to the cut-off frequency, which is expressed as:

$$\frac{V_S}{10f_{\text{max}}} \le h_{\text{max}} \le \frac{V_S}{8f_{\text{max}}} \tag{3}$$

where V_S is the shear wave velocity of the soil layer, and f_{max} is the cut-off frequency, which is 25 Hz in this paper. Accordingly, the vertical size of the grid is taken to be 0.8 - 5.0 m, and the horizontal size is taken to be 0.8 - 3.0 m, and the grids in the adjacent raft area are refined.

Huo et al. (2005) believed that ignoring the slip between the underground structure and the surrounding soil is conservatively safe, thus it is proper to bind each face of the raft to the surrounding soil in contact by binding constraints (denoted as Tie in ABAQUS). The piles are embedded into the raft and the soils for the reinforcement of the site.

4 DYNAMIC CALCULATION METHOD

4.1 Selection of bedrock motion

According to the engineering geology report of the proposed nuclear power plant site and the results of the seismic safety evaluation of the site based on the deterministic and probabilistic method, two seismic design levels of the AP1000 NPP are selected, i.e., the horizontal peak ground accelerations (PGA) at seismic bedrock interface are SL-1 (0.10 g) and SL-2 (0.20 g). To study the impact of earthquake motion characteristics on the seismic response of the NI, three records of near-field, mid-field, and far-field earthquakes were selected. The acceleration time histories and Fourier spectrum of the seismic records (SL-1) are shown in Figure 5. The information of the original records is listed in Table 3. For each seismic record, two levels of PBA (0.10 g and 0.20 g) are produced by scaling, and input on the bottom of the model along the X direction (the direction of the long side of the raft).

4.2 Dynamic response function

ABAQUS/Explicit uses an explicit central difference time domain integration algorithm to solve dynamic equations. The acceleration vector \boldsymbol{a} at the starting time t can be calculated using the following equation:

$$\ddot{\mathbf{u}}^{(i)} = \mathbf{M}^{-1} (\mathbf{F}^{(i)} - \mathbf{I}^{(i)})$$
(4)

where $\ddot{\mathbf{u}}$ is the acceleration vector; \mathbf{M} is the lumped mass matrix, \mathbf{F} is the applied load vector, \mathbf{I} is the vector of internal force, the superscript i refers to the i_{th} incremental step in an explicit dynamic analysis. In this study, the maximum time step size is set to be 10^{-5} s to achieve good convergence in the high nonlinearity of the dynamic response analysis.

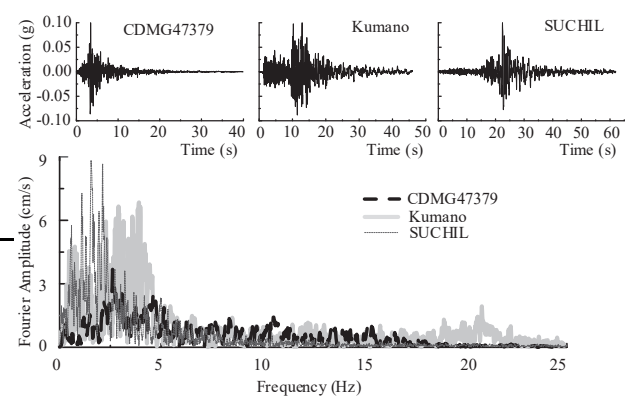


Figure 5 acceleration time histories and Fourier amplitude spectra of the input bedrock motions (SL-1 level)

Table 3 Earthquake record information

Earthquake event, date	Magnitude (Ms)	Station code	Epicenter distance (km)	Component	Predominant Period (Tp)
LOMA PRIETA, 1989	6.9	CDMG47379	11.2	EW	0.43
KUMANO, 2016	6.5	MIE015	68	$\mathbf{E}\mathbf{W}$	0.32
MICHOACAN, 1985	8.1	SUCHIL	226.4	$\mathbf{E}\mathbf{W}$	0.60

5 SEISMIC RESPONSE OF THE SOIL-PILE-RAFT FOUNDATION-NUCLEAR ISLAND SYSTEM

To investigate the overall seismic response of the NI structure, take the representative nodes at different elevations of the containment and shield buildings as observation nodes. Due to the complexity of the soil-pile-raft foundation-AP1000 NI structure system, this article only gives the seismic response of the containment and shield buildings in the X-direction considering the SPSI effect.

5.1 Spectral acceleration

Figure 6 shows the normalized spectral acceleration β of the 5% damping ratio at the observation nodes: 80, 160, 310 of the shield building and Node 500 of the bottom of the NI. It can be found that: \bigcirc The period corresponding to the peak of the β spectrum of each observation node of the shield building is the same as the predominant period of the input bedrock motion; ② When the near-field CDMG47379 is loaded, the β spectrum curves of the observing nodes of the shield building show a double peak phenomenon for both intensities. The period of the main peak is about 0.4~0.5s, and the period of the secondary peak is about 0.1~0.2s. The β spectrum values of the observation points are all smaller than that of the bedrock. When the period is less than 0.30s, the high-frequency components are significantly weakened, it may due to the existence of multiple soft soil layers which would lead to a great filter phenomenon; 3 When it under the MIE015 motion, the peak value of the β spectrum of the shield building in a period of $0.25 \sim 0.50$ s is larger than that of input bedrock motion because the predominant period of MIE015 is 0.32 s, which is close to the fundamental period of the main structure of the NI (0.34 s, the corresponding to the fundamental vibration frequency 2.91 Hz); ④ As to the SUCHIL motion, the β spectrum of the shield building at each observation point and the bottom of the NI is consistent with that of the input bedrock motion. It can be seen that the far-field wave has little effect on the containment.

5.2 Peak acceleration

The peak acceleration amplification factor (PAAF) of each observation node of containment and shield building is defined as the ratio of the peak acceleration of the observation point to that of the bedrock ground motion. The change of PAAFs with the elevation is shown in Figure 7.

The PAAFs of the containment and shield buildings all grow with the increase of their elevation. The PAAFs of Node 500 at the bottom of the NI are the largest in the case of far-field SUCHIL, the case of the near-field CDMG47379 comes second, and the case of middle-field MIE015, the values are the smallest. At the top of the containment and shield buildings, the PAAFs subjected to SUCHIL are similar to those subjected to CDMG47379, and the PAAFs for the cases under MIE015 are slightly less. This shows that the influence, which is caused by earthquakes with different dynamic characteristics, on the seismic response of the soil-pile-raft foundation- NI structure system is very complicated. Regardless of the effects of different epicenter distances, it can be noticed the larger the PBA is, the

smaller the PAAFs of the NI structure are, which indicates that the nonlinear seismic effect of the pile-raft-foundation-NI system on soft soils increases with the increase of PBA. The PAAFs of the containment and the shield buildings with elevation are quite different since they are two separate structures with differences in structural materials, cross-sectional properties.

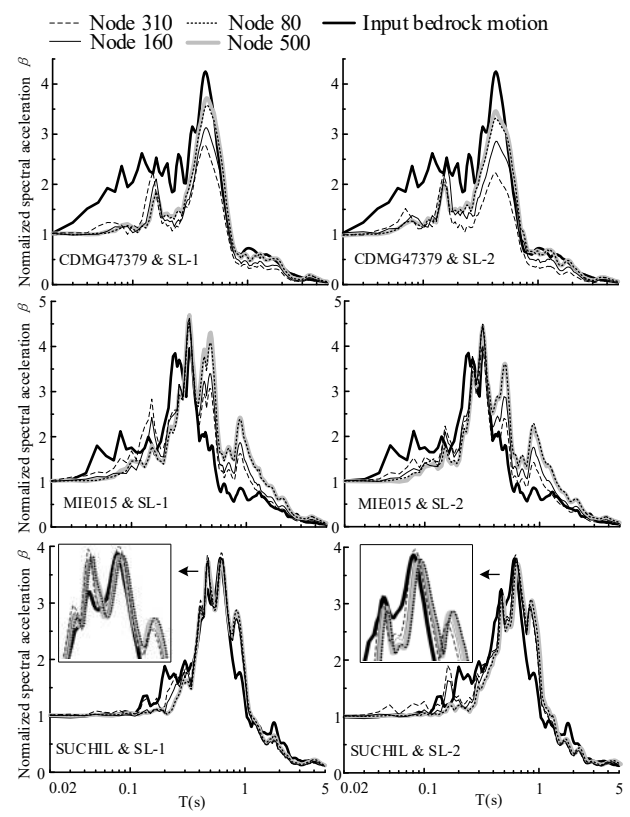


Figure 6 Normalized spectral acceleration β (5% damping) at the different observation nodes of the shield building.

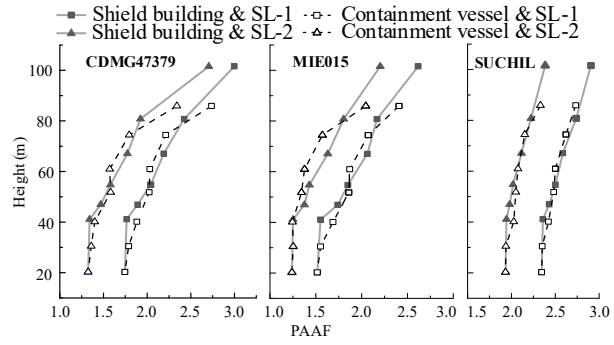


Figure 7 PAAFs at different observation nodes of the nuclear island structure elevations.

5.3 Peak relative displacement

It is assumed the horizontal peak displacement relative to the NI structure bottom is an indicator of the magnitudes of horizontal seismic responses for the NI structure.

Figure 8 depicts the variation of the absolute values of X-direction peak relative displacements (abbreviated as PRDs) of the containment and shield building subjected to earthquake motions. It can be found that the peak relative displacement of the NI structure increases with the increase of the elevation, besides the magnitude of the PRD is related to the characteristics of the input motion. When the far-field earthquake motion (SUCHIL) with rich low frequency is loaded, the PRDs are the largest, and the middle-field MIE015 comes the second, which are slightly larger than those of the cases under CDMG47379.

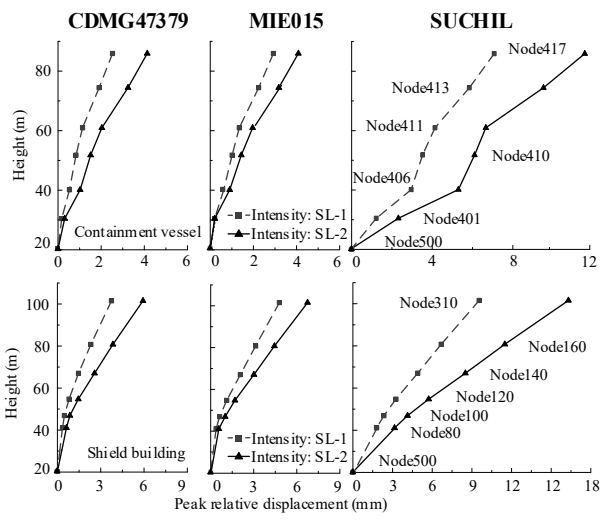


Figure 8 Absolute values of the PDRs at the observation points of the containment vessel and shield building relative to the bottom Node 500 of the nuclear island.

6 CONCLUSIONS

Aiming at a proposed AP1000 NI structure, a three-dimensional finite element model of the soft soil-pile-raft foundation-AP1000 NI structure system was established. Considering the nonlinear characteristics of soil, the seismic response characteristics of NI structure under different earthquakes are analyzed. The main conclusions are as follows:

- (1) The period corresponding to the peak of the β spectrum of each shield building observation node is the same as the predominant period of the corresponding input bedrock motion, and the shapes of β spectra at different elevations are the same for each earthquake. In the case of the near-field earthquake, the β spectrum values of the observation points are all smaller than those of the input bedrock motion. When the predominant period of the input bedrock motion is close to the fundamental period of the main structure of the NI, the β spectrum response of the NI structure in the adjacent interval of this period is greater.
- (2) The PAAFs of the NI structure increase with the height, while the variation characteristics of the two are slightly different. The greater the PBA is, the stronger the nonlinear seismic effect of soil-pile-raft foundation-NI structure system is, yet the smaller the PAAFs of the NI structure are. For the near-field and far-field strong earthquakes, respectively, the acceleration amplification effect of the NI structure derives from the NI structure itself and the seismic wave propagating through the soil layers.
- (3) The PRDs of the NI structure relative to the bottom increases with the increase of height and PBA, and the maximums appear in the cases of the far-field strong earthquake, which are followed by the middle-field strong earthquake, and the minimums are under near-field strong earthquake.

7 REFERENCES

- Chen, G. X., Ruan, B., Zhao, K., Chen, W.Y., Zhuang, H.Y., Du, X.L., Khoshnevisan, S., and Juang, C.H. 2020. Nonlinear Response Characteristics of Undersea Shield Tunnel Subjected to Strong Earthquake Motions. Journal of Earthquake Engineering 24(3), 351 - 380
- Housner, G.W. 1957. Dynamic pressure on accelerated fluid containers. Bulletin of the Seismological Society of America 1(47), 15 35.
- Huo, H., Bobet, A., Fernández, G., and Ramirez, J. 2005. Load Transfer Mechanisms between Underground Structure and Surrounding Ground: Evaluation of the Failure of the Daikai Station. Journal of Geotechnical & Geoenvironmental Engineering 131(12), 1522 -1533.
- Kuhlemeyer, R.L., and Lysmer, J. 1973. Fine element method accuracy for wave propagation problems. Journal of Soil Mechanics & Foundations Div 99(5), 421 - 427.
- Leonardo, T.S., Richard, S.O., Sener, T., and Diego, P.R. 2007. Finite element modeling of the AP1000 nuclear island for seismic analyses at generic soil and rock sites. Nuclear Engineering and Design 237(12-13), 1474 1485.
- Li, F.R., and Chen, G.X. 2020. Nonlinear seismic response characteristics of CAP1400 nuclear island structure on soft rock sites. Science and Technology of Nuclear Installations 2020, 8867026. DOI: 10.1155/2020/8867026
- Liu, J.B., and Li, B. 2005. A unified viscous-spring artificial boundary for 3-D static and dynamic applications. Science in China Series E-Technological Sciences 48 (5), 570 - 584.
- Liu, J.B., Gu, Y., and Du, Y.X. 2006. Consistent viscous-spring artificial boundaries and viscous-spring boundary elements. Chinese Journal of Geotechnical Engineering 28(9), 1070 - 1075 (in Chinese).
- Miao, Y., Yao, E., Ruan, B., and Zhuang, H.Y. 2018. Seismic response of shield tunnel subjected to spatially varying earthquake ground motions. Tunneling and Underground Space Technology 77, 216 -226.
- Ruan, B., Zhao, K., Wang S.Y., Chen, G.X., and Wang, H.Y. 2019. Numerical modeling of seismic site effects in a shallow estuarine bay (Suai Bay, Shantou, China). Engineering Geology 260, 105233. DOI: 10.1016/j.enggeo.2019.105233
- Saxena, N., and Paul, D.K. 2012. Effects of embedment including slip and separation on seismic SSI response of a nuclear reactor building. Nuclear Engineering and Design 247, 23 33.
- Wang, X.X., Zhou, Q., Zhu, K.X., Shi, L., Li, X.T., and Wang, H.T. 2017. Analysis of Seismic Soil-Structure Interaction for a Nuclear Power Plant (HTR-10). Science and Technology of Nuclear Installations 2017, 2358403. DOI: 10.1155/2017/2358403
- Wang Z.L., and Yang D. 2013. Numerical simulation of dynamic response of nuclear island under seismic load. Rock and Soil Mechanics 34(2), 400 - 406. (in Chinese)
- Westinghouse Electric Co. LLC. 2011. Westinghouse AP1000 Design Control Document. Revision17. Butler County, Pennsylvania, USA
- Yin, X.Q., Jin, Y.H., and Wang, G.X. 2017. Seismic response analysis of nuclear island buildings considering soil-structure interaction and nonlinear soil foundation. Rock and Soil Mechanics 38(4), 1114 -1120. (in Chinese)
- Zhao, C.F., and Chen, J.Y. 2014. Dynamic characteristics of AP1000 shield building for various water levels and air intakes considering fluid-structure interaction. Progress in Nuclear Energy 70, 176 - 187.
- Zhao, D.F., Ruan, B., Chen, G.X., Xu, L.Y., and Zhuang, H.Y. 2017.
 Validation of modified irregular loading-unloading rules based on Davidenkov skeleton curve and its equivalent shear strain algorithm implemented in ABAQUS. Chinese Journal of Geotechnical Engineering 39(5), 888 895. (in Chinese)